An Efficient V2X Based Vehicle Localization Using Single RSU and Single Receiver

IEEE Access
Multidisciplinary | Rapid Review | Open Access Journal

Received March 15, 2019, accepted April 3, 2019, date of publication April 10, 2019, date of current version April 17, 2019.

Digital Object Identifier 10.1109/ACCESS.2019.2909796

An Efficient V2X Based Vehicle Localization Using Single RSU and Single Receiver

SUGANG MA[1], FUXI WEN[2], (Member, IEEE), XIANGMO ZHAO[1], ZHONG-MIN WANG[3], AND DIANGE YANG[4]

[1]School of Information Engineering, Chang'an University, Xi'an 710064, China
[2]Department of Electrical Engineering, Chalmers University of Technology, 412 96 Gothenburg, Sweden
[3]School of Computer Science and Technology, Xi'an University of Posts and Telecommunications, Xi'an 710121, China
[4]State Key Laboratory of Automotive Safety and Energy, Department of Automotive Engineering, Tsinghua University, Beijing 100084, China

Corresponding authors: Xiangmo Zhao (xmzhao@chd.edu.cn) and Diange Yang (ydg@mail.tsinghua.edu.cn)

This work was supported in part by the International Science and Technology Cooperation Program of China under Contract 2016YFE0102200, in part by the State Key Laboratory of Automotive Safety and Energy under Project KF1804, in part by the European Commission H2020-MSCA-IF-2015 under Project 700044, and in part by the Science and Technology Innovation Project of Shaanxi Province under Grant 2016KTZDGY04-01.

ABSTRACT High accuracy vehicle localization information is critical for intelligent transportation systems and future autonomous vehicles. It is challenging to achieve the required centimeter-level localization accuracy, especially in urban or global navigation satellite system denied environments. Here we propose a vehicle-to-infrastructure (V2I)-based vehicle localization algorithm. First, it is low-cost and hardware requirements are simplified, the minimum requirement is a single roadside unit and single on-board receiver. Second, it is computationally efficient, the available V2I information is formulated as an over-determined system. Then, the vehicle position is estimated in a closed-form manner via the widely used weighted linear least squares (WLLS) method and meter level accuracy is achievable. Furthermore, the numerical performance of WLLS is consistent with the theoretical results in larger signal-to-noise ratio region.

INDEX TERMS Vehicle localization, vehicle-to-everything (V2X), vehicle-to-infrastructure (V2I), roadside unit (RSU), linear least squares.

I. INTRODUCTION

As sub-classes of Vehicular ad hoc networks (VANET), intelligent transport systems and connected vehicles require precise and real time vehicle positions, which creates the requirements for efficient and accurate vehicle localization [1]. Global navigation satellite system (GNSS) is one of the most commonly used vehicle localization techniques. However, it suffers from poor reliability, especially in urban environments [2]. Although real-time kinematic method can achieve centimeter level accuracy, the signal availability remains a problem. On the other hand, signal availability could be improved by combining multiple satellite navigation systems to increase the number of available satellites [3]. Furthermore, GNSS is often integrated with inertial measurement unit (IMU) to design a hybrid localization system. This IMU information can be used for moving vehicle self-localization. The vehicle position relative to its initial position can be estimated by dead reckoning. However, it suffers from the accumulated errors as the vehicle moves [2].

For the future autonomous driving applications, both integrity and localization accuracy must be improved [4]. As a key component for the future intelligent connected vehicles, the vehicle-to-everything (V2X) services are standardized by the 3rd generation partnership project (3GPP) [5]. The V2X information from connected vehicles and fixed roadside infrastructures can be integrated to the existing localization systems cooperatively to improve both accuracy and robustness at a relatively low cost, sensing range limitations associated with on-board sensors are also addressed [6]. We first review some of the widely used V2X localization techniques: vehicle-to-vehicle (V2V), vehicle-to-feature (V2F) and vehicle-to-infrastructure (V2I).

The V2V localization techniques integrate information from adjacent connected vehicles with on-board sensing capabilities. These vehicles can be considered as virtual anchor nodes. However, these methods are GNSS dependent

The associate editor coordinating the review of this manuscript and approving it for publication was Venkata Ratnam Devanaboyina.

and inter-vehicle range/angle measurements are required as well to apply the trilateration or triangulation techniques. However, the inter-vehicle measurements are sensitive to the shadowing effects either from other vehicles or from the body of the car itself.

Recently, V2F based autonomous vehicle's self-localization become more popular due to the availability of locally and globally dynamic high definition (HD) map and development of light detection and ranging (LiDAR) technologies [7]. The detected features are used as reference anchors for localization. While the main challenging is processing and transmission the high data volume with low latency [8], [9]. On the other hand, an offline map is not required if the non-cooperative features can be detected and jointly localized by the connected vehicles [10]. However, perfect association between vehicle measurements and sensed features is required.

Besides HD maps, roadside infrastructures also provide useful vehicle position information. Base station and roadside unit (RSU) are widely used facilities for V2I communications. 5G technology presents a new paradigm to provide connectivity and high data-rate services to vehicles. Using the existing communication hardware, it also provides opportunities for accurate vehicle localization from a single 5G base station [11]. To achieve this, large bandwidth combined with large scale antennas are required at both the base station and vehicle sides [12], [13]. RSU is another GNSS-free and low-cost infrastructure for localization. Each vehicle estimates its position by extracting the position related information from the radio signals transmitted by the nearby RSUs with known position [14].

RELATED WORK AND CONTRIBUTIONS

Here we focus on vehicle-to-RSU based localization. To reduce deploying costs, RSUs are often sparsely distributed and limit the application of the trilateration and triangulation-based techniques, which requires multiple RSUs to obtain location estimates. Consequently, single RSU based localization techniques have been developed recently in the literature.

An inertial navigation system (INS)-assisted and single RSU based vehicle localization framework is proposed in [15]. While two types of RSU at the entry points and the middle of the road are needed to determine the vehicle driving direction. Recently, a single RSU based localization approach using angle-of-arrival and range information between vehicle and RSU is proposed in [16]. However, multiple calibrated receivers either from the RSU or vehicle side are required to obtain an accurate angle information. Other positioning techniques are proposed in [17] and [18] by exploiting the angle information between vehicle and RSU, in conjunction with velocity vector and the broadcast RSU position. Again multiple receivers are required to estimate the angle information from the received radio signals.

The constraint of using single RSU and single on-board receiver for vehicle localization poses a significant challenge and limits the applications of the existing RSU-based localization techniques. In this paper, an IMU-assisted single RSU and single on-board receiver-based localization algorithm is proposed to eliminate this challenge.

TABLE 1. Brief comparison of the existing RSU-based localization algorithms.

	Number of RSUs	Number of Receivers
[15]	Multiple	Single
[16]	Single	Multiple
[17], [18]	Single	Multiple
Proposed	Single	Single

Our contributions are summarized as follows:

- *Low-Cost and Low Complexity:*
  Hardware requirements are simplified, the minimum requirement is a single roadside unit (RSU) and single on-board receiver.
- *Computationally Efficient:*
  The available vehicle-to-RSU information is reformulated as an over-determined system, which can be solved in a closed-form manner by the widely used linear least squares (LLS) or weighted LLS (WLLS) methods.
- *Theoretical Analysis:*
  The theoretical analysis for WLLS are carried out, if the error of extracted range information is Gaussian distributed with zero means. Furthermore, the theoretical root means square position error (RMSE) performance is provided.

The rest of the paper is organized as follows. In Section II, the problem is formulated. In Section III, we derive the proposed LLS and WLLS estimators-based vehicle localization approaches. The RMSE of the proposed algorithm is analyzed in Section IV. Simulation results are provided in Section V to evaluate the localization accuracy of the proposed localization algorithm. And conclusions are drawn in Section VI.

II. PROBLEM FORMULATION

Localization in wireless sensor networks is the process of finding a target node's absolute position using single or multiple anchor nodes. The positions of the anchor nodes are known [19]. As shown in Fig. 1, trilateration and triangulation are the widely techniques for radio-based localization by exploiting range and/or angle information between the anchor and target nodes [19]. Received signal strength (RSS) time-of-arrival (TOA), time difference-of-arrival (TDOA) and angle-of-arrival (AOA) of the emitted signals are commonly used measurements for radio-based location [20]. Basically, TDOA requires multiple synchronized anchor nodes and AOA requires multiple calibrated receivers on the target nodes [20].

In this paper, we consider the vehicle localization problem by exploiting V2I information. The vehicle trajectory can be arbitrary and within the communication range of a RSU with fixed position $\boldsymbol{p} = [x \;\; y]^T$ for 2D scenarios. The position information and ID of RSU are broadcast to the vehicle.

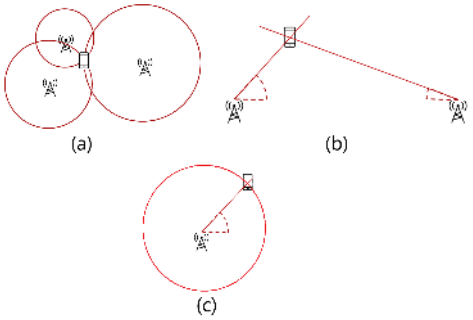

FIGURE 1. An illustration of 2D localization (a) trilateration, (b) triangulation, (c) range and angle (hybrid).

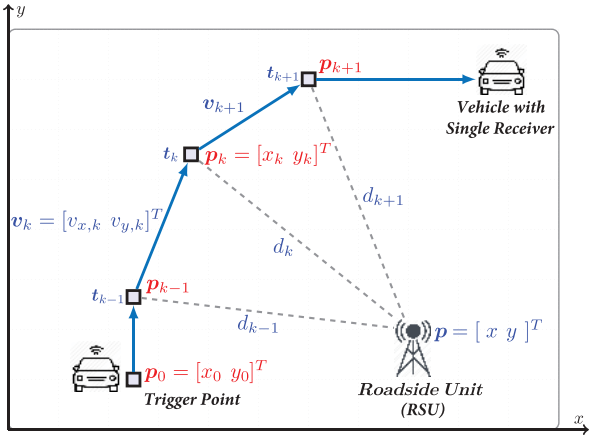

FIGURE 2. Single roadside unit and single receiver based GNSS-free vehicle localization. **Legend:** Variables in BLUE and RED colors denote the available noisy measurements and the unknown parameters to be estimated, respectively.

We assume that the vehicle velocity remains constant during very short time intervals. Let $\boldsymbol{v}_{k+1} = [v_{x,k+1}\ v_{y,k+1}]^T$ be the vector velocity during $t \in (t_k, t_{k+1}]$, which can be obtained from on board sensors at time t_k [21]. As shown in Fig. 2, $\boldsymbol{p}_k = [x_k\ \ y_k]^T$ denotes the vehicle position at time t_k. The processing of localization is triggered at time t_0 and $\boldsymbol{p}_0 = [x_0\ y_0]^T$.

Remark 1: Even though 2D localization problem is discussed in detail, extension to 3D scenarios are straightforward by setting RSU position $\boldsymbol{p} = [x\ y\ z]^T$, vehicle velocity vector $\boldsymbol{v}_{k+1} = [v_{x,k+1}\ \ v_{y,k+1}\ \ v_{z,k+1}]^T$, and the unknown vehicle position $\boldsymbol{p}_k = [x_k\ y_k\ z_k]^T$.

For the proposed two-step method, we first formulated the available vehicle-to-RSU information as an over-determined system. Then the vehicle position is estimated in a closed-form manner via the widely used linear least squares method.

III. PROPOSED LOCALIZATION ALGORITHM

Let d_k be the range information between the vehicle and RSU at time t_k. After obtaining the vector velocity $\boldsymbol{v}_k = [v_{x,k}\ \ v_{y,k}]^T$, unknown vehicle position $\boldsymbol{p}_k$ can be described as

$$\boldsymbol{p}_k = \boldsymbol{p}_{k-1} + \boldsymbol{v}_k \tau_k \Rightarrow \begin{cases} x_k = x_{k-1} + v_{x,j}\tau_k \\ y_k = y_{k-1} + v_{y,j}\tau_k \end{cases}, \tag{1}$$

where the kth time interval $\tau_k = t_k - t_{k-1}$.

It is straightforward to adopt the following kinematic model from (1),

$$\begin{cases} x_k = x_0 + \sum_{j=1}^{k} v_{x,j}\tau_j = x_0 + \Delta x_k \\ y_k = y_0 + \sum_{j=1}^{k} v_{y,j}\tau_j = y_0 + \Delta y_k \end{cases}, \tag{2}$$

where k is the number of measurements can be used for vehicle localization, the corresponding accumulated range information is defined as,

$$\Delta x_k = \sum_{j=1}^{k} v_{x,j}\tau_j \ \text{ and } \ \Delta y_k = \sum_{j=1}^{k} v_{y,j}\tau_j. \tag{3}$$

Remark 2: Assuming that from the trigger point, vehicle velocity vectors $\boldsymbol{v}_k$ and τ_k are known up to k. After obtaining trigger position, vehicle positions $\{\boldsymbol{p}_1, \boldsymbol{p}_2, \cdots, \boldsymbol{p}_k\}$ can be inferred from $\boldsymbol{p}_0$ via (2). The unknown parameters to be estimated is $\boldsymbol{p}_0 = [x_0\ \ y_0]^T$.

The range d_k between RSU and vehicle is

$$(x_k - x)^2 + (y_k - y)^2 = d_k^2. \tag{4}$$

Substituting (2) into (4) yields

$$(x_0 + \Delta x_k - x)^2 + (y_0 + \Delta y_k - y)^2 = d_k^2. \tag{5}$$

Let

$$R_0 = x_0^2 + y_0^2 \ \text{ and } \ R = x^2 + y^2, \tag{6}$$

we expand (5) to obtain

$$\begin{aligned} &2\big(\Delta x_k - x\big)x_0 + 2\big(\Delta y_k - y\big)y_0 + R_0 \\ &\qquad = d_k^2 - (\Delta x_k - x)^2 - (\Delta y_k - y)^2. \end{aligned} \tag{7}$$

Equation (7) can be rewritten as

$$\mathbf{A}\boldsymbol{\theta} = \mathbf{b}, \tag{8}$$

where

$$\mathbf{A} = \begin{bmatrix} 2(\Delta x_1 - x) & 2(\Delta y_1 - y) & 1 \\ \vdots & & \\ 2(\Delta x_j - x) & 2(\Delta y_j - y) & 1 \\ \vdots & \vdots & \vdots \\ 2(\Delta x_k - x) & 2(\Delta y_k - y) & 1 \end{bmatrix} = \begin{bmatrix} \mathbf{a}_1 \\ \vdots \\ \mathbf{a}_j \\ \vdots \\ \mathbf{a}_k \end{bmatrix} \tag{9}$$

$$\boldsymbol{\theta} = \begin{bmatrix} x_0 & y_0 & R_0 \end{bmatrix}^T = \begin{bmatrix} x_0 & y_0 & x_0^2 + y_0^2 \end{bmatrix}^T \tag{10}$$

$$\mathbf{b} = \begin{bmatrix} d_1^2 + Q_1 - R \\ \vdots \\ d_j^2 + Q_j - R \\ \vdots \\ d_k^2 + Q_k - R \end{bmatrix} = \begin{bmatrix} b_1 \\ \vdots \\ b_j \\ \vdots \\ b_k \end{bmatrix} \tag{11}$$

and for $j = 1, 2, \cdots, k$,

$$Q_j = \Delta x_j\big(2x - \Delta x_j\big) + \Delta y_j(2y - \Delta y_j). \tag{12}$$

That is, $\mathbf{A}$ is known, $\boldsymbol{\theta}$ contains the unknown parameters and $\mathbf{b}$ is the observation vector.

Remark 3: Now we extend the localization algorithm to 3D scenarios. Let $\boldsymbol{p}_k = [x_k\ y_k\ z_k]^T$ *be the 3D vehicle position. The* k*-th row of amended measurement matrix* $\mathbf{A}$ *(9) and parameter* $\boldsymbol{\theta}$ *(10) are defined as*

$$\mathbf{a}_k = \begin{bmatrix} 2(\Delta x_k - x) & 2(\Delta y_k - y) & 2(\Delta z_k - z) & 1 \end{bmatrix} \tag{13}$$

and

$$\boldsymbol{\theta} = \begin{bmatrix} x_0 & y_0 & z_0 & R_0 \end{bmatrix}^T \tag{14}$$

where $R_0 = x_0^2 + y_0^2 + z_0^2$*. Meanwhile,* R *and* Q_k *in (11) are substituted with*

$$R = x^2 + y^2 + z^2, \tag{15}$$

and

$$Q_k = \Delta x_k\big(2x - \Delta x_k\big) + \Delta y_k(2y - \Delta y_k) + \Delta z_k(2z - \Delta z_k). \tag{16}$$

A. LINEAR LEAST SQUARES (LLS)

In practice, d_j is substituted by its biased estimate $\hat{d}_j$ and is described as

$$\hat{d}_j = d_j + e_j, \quad j = 1, 2, \cdots, k, \tag{17}$$

where

$$\boldsymbol{e}_j \sim \mathcal{N}(\mu_j, \sigma_j^2) + \mathcal{N}(0, \sigma^2), \tag{18}$$

is the error component. Here, μ_j and σ_j^2 are the mean and variance of range uncertainty, and σ^2 denotes the variance of the white noise.

Substitute $\mathbf{b}$ in (8) with $\tilde{\mathbf{b}}$, we have $\mathbf{A}\boldsymbol{\theta} \approx \tilde{\mathbf{b}}$. The LLS estimate of $\boldsymbol{\theta}$ is obtained by minimizing:

$$J(\tilde{\boldsymbol{\theta}}) = \left(\mathbf{A}\tilde{\boldsymbol{\theta}} - \tilde{\mathbf{b}}\right)^T \left(\mathbf{A}\tilde{\boldsymbol{\theta}} - \tilde{\mathbf{b}}\right), \tag{19}$$

where $\tilde{\boldsymbol{\theta}}$ is the variable for $\boldsymbol{\theta}$. The closed form solution is given by

$$\hat{\boldsymbol{\theta}} = \left(\mathbf{A}^T\mathbf{A}\right)^{-1}\mathbf{A}^T\tilde{\mathbf{b}}. \tag{20}$$

The estimated trigger point is

$$\hat{\boldsymbol{p}}_0 = \begin{bmatrix} \hat{x}_0 & \hat{y}_0 \end{bmatrix}^T = \begin{bmatrix} \hat{\theta}_1 & \hat{\theta}_2 \end{bmatrix}^T. \tag{21}$$

and vehicle positions $\hat{\boldsymbol{p}}_j, \{j = 1, 2, \cdots, k\}$ can be inferred from (2).

The proposed LLS-based vehicle localization algorithm is summarized in Algorithm 1.

Algorithm 1 LLS-Based Localization

Input: $\boldsymbol{p}$, t_j, d_j and $\boldsymbol{v}_j$, for $j = 1, 2, \cdots, k$.
Output: Estimates $\hat{\boldsymbol{p}}_0$ and $\hat{\boldsymbol{p}}_j$, for $j = 1, 2, \cdots, k$.

```
for j = 1 to k do
    Calculate Δx_j and Δy_j by (3)
end for
Construct A by (9)
for j = 1 to k do
    Calculate Q_j and R by (12) and (6), respectively.
end for
Construct b by (11)
Estimate θ using LLS (20).
Estimate p̂_0 by (21) and p̂_j, j = 1, 2, ··· , k, by (2).
```

B. WEIGHTED LLS

Employing the technique proposed in [22], the LLS algorithm can be improved by including a second WLLS step by exploiting the constraint (6). Assuming that $\hat{\theta}_1$ and $\hat{\theta}_2$ of (20) is sufficiently close to x_0 and y_0, then we have

$$\begin{cases} \hat{\theta}_1^2 - x_0^2 \approx 2x_0(\hat{\theta}_1 - x_0) \\ \hat{\theta}_2^2 - y_0^2 \approx 2y_0(\hat{\theta}_2 - y_0) \end{cases} \tag{22}$$

Based on (6) and with the use of (22), we construct

$$\boldsymbol{\eta} = \mathbf{D}\mathbf{z} + \boldsymbol{r}, \tag{23}$$

where

$$\mathbf{D} = \begin{bmatrix} 1 & 0 \\ 0 & 1 \\ 1 & 1 \end{bmatrix}, \tag{24}$$

$$\mathbf{z} = \begin{bmatrix} x_0^2 & y_0^2 \end{bmatrix}^T, \tag{25}$$

$$\boldsymbol{\eta} = \begin{bmatrix} \hat{\theta}_1^2 & \hat{\theta}_2^2 & \hat{\theta}_3 \end{bmatrix}^T, \tag{26}$$

$$\boldsymbol{r} = \begin{bmatrix} 2\,x_0(\hat{\theta}_1 - x_0) & 2\,y_0(\hat{\theta}_2 - y_0) & \hat{\theta}_3 - R_0 \end{bmatrix}^T \tag{27}$$

Note that $\mathbf{z}$ is the unknown parameter to be estimated and the covariance of $\boldsymbol{r}$ is

$$\mathbf{C}_r = \begin{bmatrix} 2x_0 & & \\ & 2y_0 & \\ & & 1 \end{bmatrix} \mathbf{C}_{\hat{\boldsymbol{\theta}}} \begin{bmatrix} 2x_0 & & \\ & 2y_0 & \\ & & 1 \end{bmatrix}. \tag{28}$$

where $\mathbf{C}_{\hat{\boldsymbol{\theta}}}$ is given in (42). In practice, since x_0 and y_0 in (28) are unknown, they are substituted with $\hat{\theta}_1$ and $\hat{\theta}_2$, respectively.

The WLLS solution of $\mathbf{z}$ is

$$\hat{\mathbf{z}} = \left(\mathbf{D}^T\mathbf{C}_r^{-1}\mathbf{D}\right)^{-1}\mathbf{D}^T\mathbf{C}_r^{-1}\boldsymbol{\eta}. \tag{29}$$

As there is no Since the sign information for x_0 and y_0 cannot be recovered from $\mathbf{z}$, the improved position estimate $\hat{\boldsymbol{p}}_0$, is determined as

$$\hat{\boldsymbol{p}}_0 = \begin{bmatrix} \mathrm{sgn}(\hat{\theta}_1)\sqrt{\hat{z}_1} & \mathrm{sgn}(\hat{\theta}_2)\sqrt{\mathbf{z}_2} \end{bmatrix}^T. \tag{30}$$

where sgn represents the sign function. Again the vehicle positions $\hat{\boldsymbol{p}}_j, \{j = 1, 2, \cdots, k\}$ can be inferred from (2). The proposed method is summarized in Algorithm 2.

Algorithm 2 Weighted LLS-Based Localization

Input: $\boldsymbol{p}$, t_j, d_j and $\boldsymbol{v}_j$, for $j = 1, 2, \cdots, k$.
Output: Refined estimates $\hat{\boldsymbol{p}}_0$ and $\hat{\boldsymbol{p}}_j$, for $j = 1, 2, \cdots, k$.

1: Obtain $\hat{\boldsymbol{\theta}}$ from Algorithm 1.
2: Construct $\mathbf{h} = \mathbf{G}\mathbf{z} + \mathbf{r}$ from (23)-(27).
3: Calculate covariance matrix $\mathbf{C}_r$ by (28).
4: Estimate $\boldsymbol{z}$ using WLLS (29).
5: Obtain the refined $\hat{\boldsymbol{p}}_0$ by (30).
6: Estimate the refined $\hat{\boldsymbol{p}}_j$ for $j = 1, 2, \cdots, k$, by (2).

IV. PERFORMANCE ANALYSIS

Compared with Q_j in (11), the dominant errors are from the estimated range $\hat{d}_j$. After ignoring the error in Q_j, we have

$$\tilde{\mathbf{b}} = \mathbf{b} + \boldsymbol{w} = \left[\tilde{b}_1, \cdots, \tilde{b}_j, \cdots, \tilde{b}_k\right]^T, \tag{31}$$

where observation error

$$\boldsymbol{w} = [\boldsymbol{e}_1^2 + 2\boldsymbol{e}_1 d_1, \cdots, \boldsymbol{e}_j^2 + 2\boldsymbol{e}_j d_j, \cdots, \boldsymbol{e}_k^2 + 2\boldsymbol{e}_k d_k]^T. \tag{32}$$

Lemma 1: The mean of $\tilde{\boldsymbol{b}}$ is

$$\mathrm{E}[\tilde{\boldsymbol{b}}] = \boldsymbol{b} + \begin{bmatrix} \sigma_1^2 + \sigma^2 + \mu_1^2 + 2\mu_1 d_1 \\ \vdots \\ \sigma_j^2 + \sigma^2 + \mu_j^2 + 2\mu_j d_j \\ \vdots \\ \sigma_k^2 + \sigma^2 + \mu_k^2 + 2\mu_k d_k \end{bmatrix}, \tag{33}$$

where $E[\cdot]$ is the expectation operator. The covariance matrix of $\tilde{\boldsymbol{b}}$ is given by

$$\mathbf{C}_{\tilde{\boldsymbol{b}}} = \begin{bmatrix} c_1 & & & \\ & \ddots & & \\ & & c_j & \\ & & & \ddots \\ & & & & c_k \end{bmatrix}, \tag{34}$$

where

$$c_j = 2\left(\sigma_j^4 + \sigma^4\right) + 4d_j^2\left(\sigma_j^2 + \sigma^2\right),\ j = 1, 2, \cdots, k \tag{35}$$

Please refer to the proof provided in Appendix for more details.

A. BIAS AND MEAN SQUARE ERROR ANALYSIS

The WLLS estimate of $\boldsymbol{\theta}$ is given by

$$\hat{\boldsymbol{\theta}} = \arg\min_{\tilde{\boldsymbol{\theta}}} J(\tilde{\boldsymbol{\theta}}), \tag{36}$$

where

$$J(\tilde{\boldsymbol{\theta}}) = \left(\mathbf{A}\tilde{\boldsymbol{\theta}} - \tilde{\mathbf{b}}\right)^T \mathbf{C}_{\tilde{\boldsymbol{b}}}^{-1}\left(\mathbf{A}\tilde{\boldsymbol{\theta}} - \tilde{\mathbf{b}}\right), \tag{37}$$

and weighting matrix $\mathbf{C}_{\tilde{\boldsymbol{b}}}^{-1}$ is given in (34). Equation (36) implies that

$$\nabla\left(J(\hat{\boldsymbol{\theta}})\right) = \left.\frac{\partial J(\tilde{\boldsymbol{\theta}})}{\partial \tilde{\boldsymbol{\theta}}}\right|_{\tilde{\boldsymbol{\theta}}=\hat{\boldsymbol{\theta}}} = 0, \tag{38}$$

where $\nabla\left(J(\hat{\boldsymbol{\theta}})\right)$ denotes the gradient vector evaluated at the estimated value. If the estimation error $\hat{\boldsymbol{\theta}} - \boldsymbol{\theta}$ is sufficiently small, take first-order Taylor series expansion of (38) around $\boldsymbol{\theta}$, we have

$$\nabla\left(J(\hat{\boldsymbol{\theta}})\right) \approx \nabla\left(J(\boldsymbol{\theta})\right) + \mathbf{H}\left(J(\boldsymbol{\theta})\right)\left(\hat{\boldsymbol{\theta}} - \boldsymbol{\theta}\right), \tag{39}$$

where $\nabla\left(J(\boldsymbol{\theta})\right)$ and $\mathbf{H}\left(J(\boldsymbol{\theta})\right)$ are the Hessian matrix and gradient vector evaluated at $\boldsymbol{\theta}$, respectively. Bias is obtained by taking the expected value on (39) [23],

$$\mathrm{bias}(\hat{\boldsymbol{\theta}}) \approx -\left[\mathrm{E}\left\{\mathbf{H}\left(J(\boldsymbol{\theta})\right)\right\}\right]^{-1}\mathrm{E}\left\{\nabla\left(J(\boldsymbol{\theta})\right)\right\}. \tag{40}$$

Similarly, the covariance matrix [22] is

$$\mathbf{C}_{\hat{\boldsymbol{\theta}}} \approx \left[\mathrm{E}\left\{\mathbf{H}\left(J(\boldsymbol{\theta})\right)\right\}\right]^{-1}\mathrm{E}\left\{\nabla\left(J(\boldsymbol{\theta})\nabla^T\left(J(\boldsymbol{\theta})\right)\right\}\left[\mathrm{E}\left\{\mathbf{H}\left(J(\boldsymbol{\theta})\right)\right\}\right]^{-1}. \tag{41}$$

Apply the bias (40) and MSE (41) formulas, we obtain: $\mathrm{E}\{\boldsymbol{\theta}\} = \hat{\boldsymbol{\theta}}$ and

$$\mathbf{C}_{\hat{\boldsymbol{\theta}}} = \left(\mathbf{A}^T\mathbf{C}_{\tilde{\boldsymbol{b}}}^{-1}\mathbf{A}\right)^{-1}. \tag{42}$$

For $[x_0, y_0]^T$ the RMSE is given by

$$\mathrm{RMSE} = \sqrt{[\mathbf{C}_{\hat{\boldsymbol{\theta}}}]_{1,1} + [\mathbf{C}_{\hat{\boldsymbol{\theta}}}]_{2,2}}, \tag{43}$$

where $[\ ]_{i,j}$ denotes the (i, j) entry of a matrix.

B. CRAMÉR-RAO LOWER BOUND (CRLB)

The CRLB of $\hat{\boldsymbol{p}}_0$ is analyzed as follows. Implicitly, $\hat{\boldsymbol{p}}_0$ corresponds to minimizing (37) subject to (6). Employing (5) and (34), we can write

$$\hat{\boldsymbol{p}}_0 = \arg\min_{\tilde{\boldsymbol{p}}_0} J(\tilde{\boldsymbol{p}}_0), \tag{44}$$

where

$$J(\tilde{\boldsymbol{p}}_0) = \sum_{k=1}^{K} \frac{\left[\left(\tilde{x}_0 + \Delta x_k - x\right)^2 + \left(\tilde{y}_0 + \Delta y_k - y\right)^2 - \hat{d}_k^2\right]^2}{2\sigma_k^4 + 4d_k^2\sigma_k^2} \tag{45}$$

The Hessian matrix for $J(\tilde{\boldsymbol{p}}_0)$ is expressed as

$$\frac{\partial^2 J(\tilde{\boldsymbol{p}}_0)}{\partial \tilde{\boldsymbol{p}}_0 \partial \tilde{\boldsymbol{p}}_0^T} = \begin{bmatrix} \frac{\partial^2 J(\tilde{\boldsymbol{p}}_0)}{\partial \tilde{x}_0^2} & \frac{\partial^2 J(\tilde{\boldsymbol{p}}_0)}{\partial \tilde{x}_0 \partial^T \tilde{y}_0} \\ \frac{\partial^2 J(\tilde{\boldsymbol{p}}_0)}{\partial \tilde{y}_0 \partial^T \tilde{x}_0}\tilde{\mathrm{a}} & \frac{\partial^2 J(\tilde{\boldsymbol{p}}_0)}{\partial \tilde{y}_0^2} \end{bmatrix} = \begin{bmatrix} J_{xx} & J_{xy} \\ J_{xy} & J_{yy} \end{bmatrix}. \tag{46}$$

We start with

$$\begin{aligned} \frac{\partial J(\tilde{\boldsymbol{p}}_0)}{\partial \tilde{x}_0} = &\sum_{k=1}^{K} \frac{2\left(\tilde{x}_0 + \Delta x_k - x\right)^2(\tilde{x}_0 + \Delta x_k - x)}{\sigma_k^4 + 2d_k^2\sigma_k^2} \\ &+ \sum_{k=1}^{K} \frac{2\left(\tilde{y}_0 + \Delta y_k - y\right)^2(\tilde{x}_0 + \Delta x_k - x)}{\sigma_k^4 + 2d_k^2\sigma_k^2} \\ &- \sum_{k=1}^{K} \frac{2\hat{d}_k^2(\tilde{x}_0 + \Delta x_k - x)}{\sigma_k^4 + 2d_k^2\sigma_k^2}. \end{aligned} \tag{47}$$

Using (47), we obtain

$$J_{xx} = \sum_{k=1}^{K} \frac{2\left[3(\tilde{x}_0 + \Delta x_k - x)^2 + (\tilde{y}_0 + \Delta y_k - y)^2 - \hat{d}_k^2\right]}{\sigma_k^4 + 2d_k^2\sigma_k^2}, \tag{48}$$

$$J_{yy} = \sum_{k=1}^{K} \frac{2\left[3(\tilde{y}_0 + \Delta y_k - y)^2 + (\tilde{x}_0 + \Delta x_k - x)^2 - \hat{d}_k^2\right]}{\sigma_k^4 + 2d_k^2\sigma_k^2} \tag{49}$$

and

$$J_{xy} = J_{yx} = \sum_{k=1}^{K} \frac{4(\tilde{x}_0 + \Delta x_k - x)(\tilde{y}_0 + \Delta y_k - y)}{\sigma_k^4 + 2d_k^2\sigma_k^2}. \tag{50}$$

Evaluating these partial derivatives at $\tilde{\boldsymbol{p}}_0 = \boldsymbol{p}_0$ and employing $\mathrm{E}\{\hat{d}_k^2\} = d_k^2$ yields

$$\eta_{xx} = \mathrm{E}\{J_{xx}\} = \sum_{k=1}^{K} \frac{4(x_0 + \Delta x_k - x)^2}{\sigma_k^4 + 2d_k^2\sigma_k^2}, \tag{51}$$

and

$$\eta_{yy} = \mathrm{E}\{J_{yy}\} = \sum_{k=1}^{K} \frac{4(y_0 + \Delta y_k - y)^2}{\sigma_k^4 + 2d_k^2\sigma_k^2}. \tag{52}$$

Similarly, we get

$$\eta_{xy} = \eta_{yx} = \mathrm{E}\{J_{xy}\} = \mathrm{E}\{J_{yx}\} = \sum_{k=1}^{K} \frac{4(x_0 + \Delta x_k - x)(y_0 + \Delta y_k - y)}{\sigma_k^4 + 2d_k^2\sigma_k^2}. \tag{53}$$

Using (51), (52) and ((53)), we have

$$\mathrm{E}\left\{\frac{\partial^2 J(\tilde{\boldsymbol{p}}_0)}{\partial\tilde{\boldsymbol{p}}_0\partial\tilde{\boldsymbol{p}}_0^T}\right\}\Big|_{\tilde{\boldsymbol{p}}_0=\boldsymbol{p}_0} = \begin{bmatrix} \eta_{xx} & \eta_{xy} \\ \eta_{yx}\tilde{\mathrm{a}} & \eta_{yy} \end{bmatrix}. \tag{54}$$

V. SIMULATION RESULTS

Simulations are implemented to evaluate the WLLS (30) and LLS (21) vehicle localization algorithms, as a benchmark theoretical RMSE (43) and CRLB (54) are also included. The position of RSU is $\boldsymbol{p} = [200\ 0]^T$ and $\boldsymbol{p}_o = [1\ 2]^T$. Sampling frequencies $f_s = 10$ Hz and observation period 30 s are considered. The signal-to-noise ratio (SNR) in dB scale is defined as

$$\mathrm{SNR} = 10\log_{10}\left(d_j^2/\sigma^2\right), \tag{55}$$

where σ^2 is the variance of the Gaussian noise. Two scenarios with accurate and inaccurate range information d_j are considered.

- Accurate range information, the error component in (17) is described as $\boldsymbol{e}_j \sim \mathcal{N}(0, \sigma^2)$.
- Inaccurate range information, the error component is $\boldsymbol{e}_j \sim \mathcal{N}(\mu_j, \sigma_j^2) + \mathcal{N}(0, \sigma^2)$.

All the results are obtained by averaging over 1000 independent runs.

1) ACCURATE V2I RANGE INFORMATION

In the first test, constant velocity vector is considered and $\boldsymbol{v}_k = [v_{x,k}\ v_{y,k}]^T = [6\ 4]^T$. Fig. 3 shows the RMSE of the LLS and WLLS methods versus SNR. The theoretical variances of the position estimates of the proposed estimator and CRLB are also included. WLLS-based localization outperforms LLS-based in terms of RMSE and meter level accuracy is achievable. Furthermore, the RMSEs of WLLS agree with (42) and approach the CRLB when SNR is larger than 20 dB. As shown in Fig. 4, localization accuracy is further improved by increasing T_o and f_s, while trade-offs should be considered between computational complexity and localization accuracy.

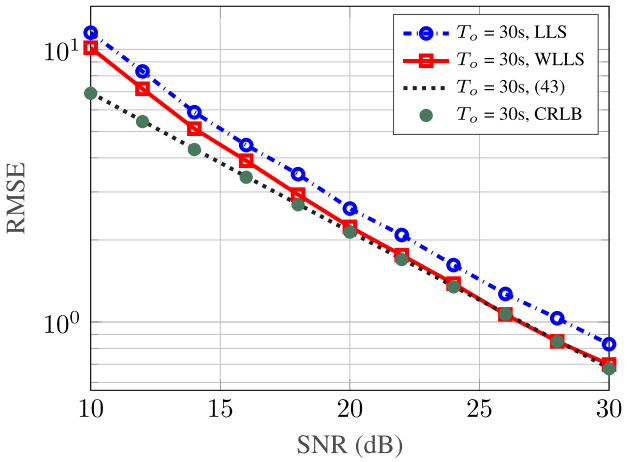

FIGURE 3. RMSE versus SNR, observation time $T_o = 30$ s and sampling frequency $f_s = 10$ Hz.

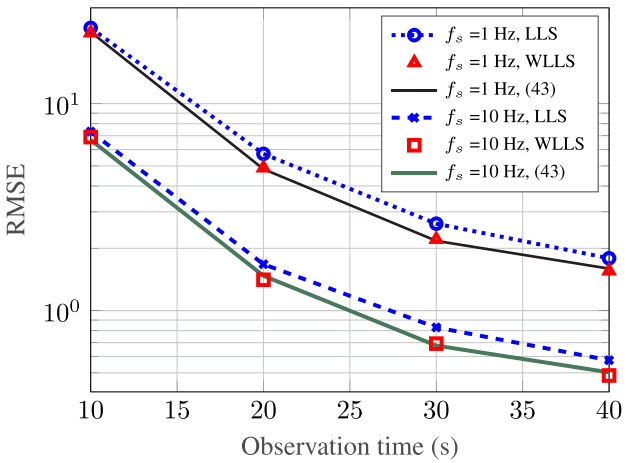

FIGURE 4. RMSE versus observation time T_o, SNR is 30 dB and different sampling frequency f_s.

2) INACCURATE V2I RANGE INFORMATION

In the second test, inaccurate V2I range information is considered and $\boldsymbol{v}_k = [v_{x,k}\ v_{y,k}]^T = [6\ 8]^T$, observation time $T_o = 30$ s and sampling frequency $f_s = 10$Hz. As shown

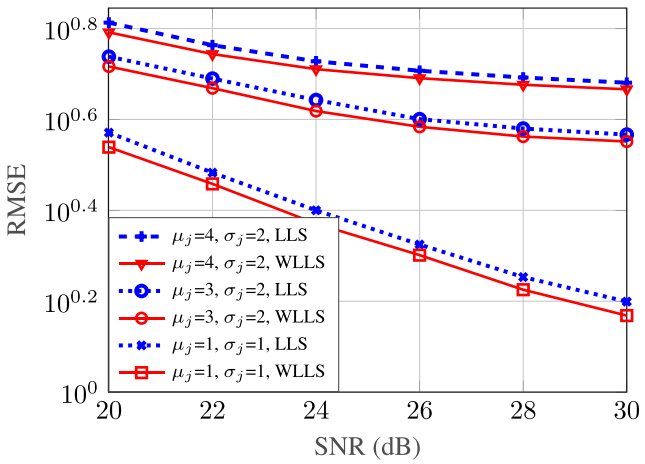

FIGURE 5. RMSE versus SNR for different μ_j and σ_j, $T_o = 30$ s and $f_s = 10$Hz.

in Fig. 5, accurate V2I range information is critical for the proposed algorithm. Larger uncertainty level of the estimated range information leads to larger RMSEs. Compared with LLs, better performance is achieved for WLLS and with a slightly higher computational complexity.

VI. CONCLUSION

We propose a low-cost, single on-board receiver and single RSU-based vehicle localization algorithm. After formulating the required V2I information into an over-determined system, vehicle positions are estimated efficiently by LLS type methods in a closed-form manner. WLLS-based localization algorithm outperforms LLS-based in terms of RMSE and meter level accuracy is achievable. Furthermore, RMSE performance of WLLS is consistent with (42) and approach the CRLB in larger SNR region. Validating the performance of the proposed technique via experimental data is one of our future works.

APPENDIX A
PROOF OF LEMMA 1

Proof: Let χ_n^2 denote the Chi-squared distribution with n degrees of freedom. $\boldsymbol{e}_j \sim \mathcal{N}(0, \sigma_j^2), j = 1, 2, \cdots, k$, is a normal random variable with zero mean and variance σ_j^2, then $\boldsymbol{e}_j^2 \sim \sigma_j^2 \boldsymbol{\chi}_1^2$.

Since the mean and variance of χ_1^2 are 1 and 2, respectively. Then we have $\mathrm{E}[\boldsymbol{e}_j^2] = \sigma_j^2$ and $\mathrm{Var}[\boldsymbol{e}_j^2] = 2\sigma_j^4$. The mean of $\tilde{\boldsymbol{b}}_j$ is

$$\mathrm{E}[\tilde{\boldsymbol{b}}_j] = \boldsymbol{b}_j + \sigma_j^2. \tag{56}$$

Equation (33) is obtained by reformulating (56) into matrix form. Since all odd-order moments of zero-mean Gaussian variables are zero, then $\mathrm{E}(\boldsymbol{e}_j) = \mathrm{E}\left(\boldsymbol{e}_j^3\right) = 0$. The variance of $\tilde{\boldsymbol{b}}_j$ is defined as

$$\begin{aligned}\mathrm{Var}[\tilde{\boldsymbol{b}}_j] &= \mathrm{E}\left[\left(\tilde{\boldsymbol{b}}_j - \mathrm{E}[\tilde{\boldsymbol{b}}_j]\right)^2\right] = \mathrm{E}\left[\left(\boldsymbol{e}_j^2 + 2d_j\boldsymbol{e}_j - \sigma_j^2\right)^2\right] \\ &= \mathrm{E}\left(\boldsymbol{e}_j^4\right) + 4d_j\mathrm{E}(\boldsymbol{e}_j^3) + 2(2d_j^2 - \sigma_j^2)\mathrm{E}(\boldsymbol{e}_j^2) \\ &\quad + 4\sigma_j^2 d_j \mathrm{E}(\boldsymbol{e}_j) + \sigma_j^4 \\ &= \mathrm{E}\left(\boldsymbol{e}_j^4\right) + 2(2d_j^2 - \sigma_j^2)\mathrm{E}(\boldsymbol{e}_j^2) + \sigma_j^4. \end{aligned} \tag{57}$$

Substituting

$$\mathrm{E}\left(\boldsymbol{e}_j^4\right) = \mathrm{Var}[\boldsymbol{e}_j^2] + \left[\mathrm{E}\left(\boldsymbol{e}_j^2\right)\right]^2 = 3\sigma_j^4, \tag{58}$$

and $\mathrm{E}[\boldsymbol{e}_j^2] = \sigma_j^2$ into (57), we have

$$\mathrm{Var}[\tilde{\boldsymbol{b}}_j] = 2\sigma_j^4 + 4d_j^2\sigma_j^2. \tag{59}$$

Now we compute the covariance of random variables $\tilde{\boldsymbol{b}}_i$ and $\tilde{\boldsymbol{b}}_j$,

$$\begin{aligned}\mathrm{Cov}[\tilde{\boldsymbol{b}}_i, \tilde{\boldsymbol{b}}_j] &= \mathrm{E}\left[\left(\tilde{\boldsymbol{b}}_i - \mathrm{E}[\tilde{\boldsymbol{b}}_i]\right)\left(\tilde{\boldsymbol{b}}_j - \mathrm{E}[\tilde{\boldsymbol{b}}_j]\right)\right] \\ &= \mathrm{E}\left[\left(\boldsymbol{r}_i^2 + 2d_i\boldsymbol{r}_i - \sigma_i^2\right)\left(\boldsymbol{r}_j^2 + 2d_j\boldsymbol{r}_j - \sigma_j^2\right)\right] \\ &= \mathrm{E}\left[\boldsymbol{r}_i^2\boldsymbol{r}_j^2\right] - \sigma_i^2\mathrm{E}\left[\boldsymbol{r}_j^2\right] - \sigma_j^2\mathrm{E}\left[\boldsymbol{r}_i^2\right] + \sigma_i^2\sigma_j^2 \\ &\quad + 2d_j\mathrm{E}\left[\boldsymbol{r}_i^2\boldsymbol{r}_j\right] + 2d_i\mathrm{E}\left[\boldsymbol{r}_i\boldsymbol{r}_j^2\right] + 4d_id_j\mathrm{E}\left[\boldsymbol{r}_i\boldsymbol{r}_j\right] \\ &\quad - 2d_i\sigma_j^2\mathrm{E}\left[\boldsymbol{r}_i\right] - 2d_j\sigma_i^2\mathrm{E}\left[\boldsymbol{r}_j\right] \\ &= \mathrm{E}\left[\boldsymbol{r}_i^2\boldsymbol{r}_j^2\right] - \sigma_i^2\sigma_j^2. \end{aligned} \tag{60}$$

Based on the Isserlis's theorem [24], we have

$$\mathrm{E}\left[\boldsymbol{r}_i^2\boldsymbol{r}_j^2\right] = \mathrm{E}[\boldsymbol{r}_i^2]\mathrm{E}[\boldsymbol{r}_j^2] + 2(\mathrm{E}[\boldsymbol{r}_i\boldsymbol{r}_j])^2 = \sigma_i^2\sigma_j^2. \tag{61}$$

Because $\boldsymbol{r}_i$ and $\boldsymbol{r}_j$ are zero mean and independent, then $\mathrm{E}[\boldsymbol{r}_i\boldsymbol{r}_j] = 0$. Substituting (61) into (60) yields $\mathrm{Cov}(\tilde{\boldsymbol{b}}_i, \tilde{\boldsymbol{b}}_j) = 0$, for $i \neq j$. Diagonal covariance matrix $\mathbf{C}_{\tilde{\boldsymbol{b}}}$ in (34) is obtained. □

ACKNOWLEDGMENT

(Sugang Ma and Fuxi Wen are co-first authors.)

REFERENCES

[1] M. Usman, M. R. Asghar, I. S. Ansari, F. Granelli, and K. A. Qaraqe, "Technologies and solutions for location-based services in smart cities: Past, present, and future," *IEEE Access*, vol. 6, pp. 22240–22248, 2018.
[2] S. Kuutti, S. Fallah, K. Katsaros, M. Dianati, F. Mccullough, and A. Mouzakitis, "A survey of the state-of-the-art localization techniques and their potentials for autonomous vehicle applications," *IEEE Internet Things J.*, vol. 5, no. 2, pp. 829–846, Apr. 2018.
[3] P. Kovár, P. Kačmarík, and F. Vejražka, "Interoperable GPS, GLONASS and galileo software receiver," *Gyroscopy Navigat.*, vol. 2, no. 2, pp. 69–74, Apr. 2011.
[4] R. Karlsson and F. Gustafsson, "The future of automotive localization algorithms: Available, reliable, and scalable localization: Anywhere and anytime," *IEEE Signal Process. Mag.*, vol. 34, no. 2, pp. 60–69, Mar. 2017.
[5] S. Chen *et al.*, "Vehicle-to-everything (v2x) services supported by LTE-based systems and 5G," *IEEE Commun. Standard Mag.*, vol. 1, no. 2, pp. 70–76, Jun. 2017.
[6] W. Tong, A. Hussain, W. X. Bo, and S. Maharjan, "Artificial intelligence for vehicle-to-everything: A survey," *IEEE Access*, vol. 7, pp. 10823–10843, 2019.
[7] E. Javanmardi, M. Javanmardi, Y. Gu, and S. Kamijo, "Factors to evaluate capability of map for vehicle localization," *IEEE Access*, vol. 6, pp. 49850–49867, 2018.
[8] H. G. Seif and X. Hu, "Autonomous driving in the iCity—HD maps as a key challenge of the automotive industry," *Engineering*, vol. 2, no. 2, pp. 159–162, 2016.
[9] K. Lee, J. Kim, Y. Park, H. Wang, and D. Hong, "Latency of cellular-based V2X: Perspectives on TTI-proportional latency and TTI-independent latency," *IEEE Access*, vol. 5, pp. 15800–15809, 2017.
[10] G. Soatti, M. Nicoli, N. Garcia, B. Denis, R. Raulefs, and H. Wymeersch, "Implicit cooperative positioning in vehicular networks," *IEEE Trans. Intell. Transp. Syst.*, vol. 19, no. 12, pp. 3964–3980, Dec. 2018.

[11] H. Wymeersch *et al.*, "5G mm wave downlink vehicular positioning," in *Proc. IEEE Global Commun. Conf. (GLOBECOM)*, Dec. 2018, pp. 206–212.
[12] H. Wymeersch, G. Seco-Granados, G. Destino, D. Dardari, and F. Tufvesson, "5G mmWave positioning for vehicular networks," *IEEE Wireless Commun.*, vol. 24, no. 6, pp. 80–86, Dec. 2017, doi: 10.1109/MWC.2017.1600374.
[13] G. Artner, W. Kotterman, G. Del Galdo, and M. A. Hein, "Automotive antenna roof for cooperative connected driving," *IEEE Access*, vol. 7, pp. 20083–20090, 2019.
[14] C.-H. Ou, "A roadside unit-based localization scheme for vehicular ad hoc networks," *Int. J. Commun. Syst.*, vol. 27, no. 1, pp. 135–150, Jan. 2012.
[15] A. Khattab, Y. A. Fahmy, and A. A. Wahab, "High accuracy GPS-free vehicle localization framework via an INS-assisted single RSU," *Int. J. Distrib. Sensor Netw.*, vol. 11, no. 5, May 2015, Art. no. 795036.
[16] R. Zhang, G. Chen, Q. Zeng, and L. Shen, "Single-site positioning method based on high-resolution estimation in VANET localization," *IEEE Access*, vol. 6, pp. 54674–54682, 2018.
[17] A. Fascista, G. Ciccarese, G. Ricci, and A. Coluccia, "A localization algorithm based on V2I communications and AOA estimation," *IEEE Signal Process Lett.*, vol. 24, no. 1, pp. 126–130, Jan. 2017.
[18] A. Fascista, G. Ciccarese, A. Coluccia, and G. Ricci, "Angle of arrival-based cooperative positioning for smart vehicles," *IEEE Trans. Intell. Transp. Syst.*, vol. 19, no. 9, pp. 2880–2892, Sep. 2018.
[19] L. N. Balico, A. A. F. Loureiro, E. F. Nakamura, R. S. Barreto, R. W. Pazzi, and H. A. B. F. Oliveira, "Localization prediction in vehicular ad Hoc networks," *IEEE Commun. Surv. Tuts.*, vol. 20, no. 4, pp. 2784–2803, 4th quart., 2018.
[20] F. Gustafsson and F. Gunnarsson, "Mobile positioning using wireless networks: Possibilities and fundamental limitations based on available wireless network measurements," *IEEE Signal Process. Mag.*, vol. 22, no. 4, pp. 41–53, Jul. 2005.
[21] J. J. Oh and S. B. Choi, "Vehicle velocity observer design using 6-D IMU and multiple-observer approach," *IEEE Trans. Intell. Transp. Syst.*, vol. 13, no. 4, pp. 1865–1879, Dec. 2012.
[22] H. C. So and L. Lin, "Linear least squares approach for accurate received signal strength based source localization," *IEEE Trans. Signal Process.*, vol. 59, no. 8, pp. 4035–4040, Aug. 2011.
[23] H. C. So, Y. T. Chan, K. Ho, and Y. Chen, "Simple formulae for bias and mean square error computation [DSP tips and tricks]," *IEEE Signal Process. Mag.*, vol. 30, no. 4, pp. 162–165, Jul. 2013.
[24] L. Isserlis, "On a formula for the product-moment coefficient of any order of a normal frequency distribution in any number of variables," *Biometrika*, vol. 12, nos. 1–2, pp. 134–139, 1918.

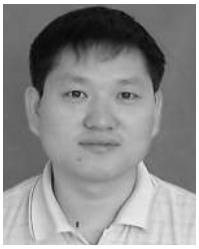

SUGANG MA is currently pursuing the Ph.D. degree in computer science with Chang'an University. He is currently a Senior Engineer with the Xi'an University of Posts and Telecommunications. His current research interests include computer vision and machine learning. He is a Senior Member of the China Communications Society.

FUXI WEN received the Ph.D. degree in electrical and electronic engineering from Nanyang Technological University, Singapore, in 2013. He held several research positions in Singapore and U.K., from 2013 to 2017. He has been a Marie Skodowska-Curie Fellow with the Department of Electrical Engineering, Chalmers University of Technology, Sweden, since 2017. His research interests include signal processing, 5G localization, vehicle-to-everything, and their applications in intelligent and connected vehicles.

He is a member of the IEEE Signal Processing Society, the IEEE Vehicular Technology Society, and the International Society of Information Fusion. He currently serves as the Secretary for the IEEE Signal Processing Society Sweden chapter, a Guest Editor for a Special Issue on Digital Signal Processing.

XIANGMO ZHAO was with Chang'an University for more than 20 years, where he is currently the Vice President and the Director of the Science and Technology Innovation Team of Multi-sources Traffic Information Sensing and Fusion, Ministry of Education, and also a Professor with the School of Information Engineering. He has published more than 200 peer-reviewed papers. His research interests include the Internet of Vehicles, testing of intelligent vehicles, intelligent transportation systems, and nondestructive testing for road infrastructures. He currently serves as a member of the State Council's Discipline Evaluation Committee on Transportation Engineering, and is sitting as the academic leader of state-level key discipline of the Traffic Information Engineering and Control in Chang'an University. He received the National SciTech Progress Awards twice for his contribution on promoting the development of indoor vehicle testing technology in China. He also received the National May 1st Labor Medal of China, in 2001.

ZHONG-MIN WANG received the M.S. degree in mechatronic engineering and the Ph.D. degree in mechanical manufacture and automation from the Beijing Institute of Technology, Beijing, China, in 1993 and 2000, respectively. He was with Xidian University, from 1993 to 1997. From 2004 to 2005, he was a Visiting Scholarship with the Robotics Laboratory, The Australian National University, Canberra, Australia. Since 2000, he has been a Full Professor with the School of Computer Science and Technology, Xi'an University of Posts and Telecommunications.

His current research interests include embedded intelligent perception, intelligent information processing, machine learning, brain–computer interface, and effective computing.

DIANGE YANG received the B.S. and Ph.D. degrees from Tsinghua University, in 1996 and 2001, respectively, where he is currently a Professor with the Department of Automotive Engineering. He is also the Head of the Department of Automotive Engineering. His current research interests include intelligent connected vehicles and autonomous driving.

He has authored 12 software copyrights and registered more than 60 national patents, he also published 120 papers. He has received numerous awards during his career, including the Excellent Young Scientist of Beijing, in 2010 and the Distinguished Young Science Technology Talent of Chinese Automobile Industry, in 2011. He is also a recipient of the Second Prize of National Technology Invention Rewards of China, in 2010 and 2013.